

Co-existence of Epithelioid and Fibroblastoid Subsets in a Sarcomatoid Renal Carcinoma Cell Line Revealed by Clonal Studies

CHIN-HSUAN HSIEH¹, HUNG-CHANG CHEN¹, YING-HSU CHANG³, SEE-TONG PANG^{2,3},
MING-LING KUO^{1,4*}, CHENG-KENG CHUANG^{2,3} and SHUEN-KUEI LIAO^{5,6,7*}

¹Graduate Institute of Biomedical Sciences, ²School of Medicine, and ⁴Department of Microbiology and Immunology, College of Medicine, Chang Gung University, Taoyuan, Taiwan, R.O.C.;

³Division of Uro-oncology, Department of Surgery, Chang Gung Memorial Hospital, Taoyuan, Taiwan, R.O.C.;

⁵Graduate Institute of Cancer Biology and Drug Discovery and

⁶Center of Excellence for Cancer Research, Taipei Medical University, Taipei, Taiwan, R.O.C.;

⁷R&D Division, Vectorite Biomedica Inc., Taipei, Taiwan, R.O.C.

Abstract. *Background:* The biology of sarcomatoid renal cell carcinoma (RCC) and its conversion from and to the clear cell RCC are not fully-understood. We aimed to analyze the sarcomatoid RCC cell line, RCC52, derived from a lymph node metastatic lesion consisting mostly of sarcomatoid RCC cells with occasional clear cell areas. *Materials and Methods:* Representative clonal epithelioid and fibroblastoid sublines isolated from the RCC52 cell line were analyzed alongside the parental line. Cytofluorometric and western blot analyses were used for phenotypic study. Xenotransplantation and in vitro invasive assays were used to determine tumorigenicity and invasiveness. Immunohistology in conjunction with antibodies to paired box gene-2 (PAX2) were used to determine if xenografts or tumor biopsies had the clear cell component. *Results:* RCC52 cells grown as monolayers in vitro were all PAX2-negative, and consisted mostly of epithelioid cells and partly of fibroblastoid cells as noted in a previous study, confirming the co-existence of these two cell types in the in vitro growth of exclusive sarcomatoid RCC cells. Immunohistology revealed that the parental line and all epithelioid sublines tested were able to develop into solid tumors consisting mostly of sarcomatoid cells with PAX2-positive clear cells in some areas. The RCC stem cell marker

CD105 was selectively expressed by a small proportion of the epithelioid, but not fibroblastoid, sublines, which was in line with the tumorigenic property of the epithelioid sublines containing cancer stem cells (CSCs). In contrast, only fibroblastoid sublines exhibited migratory/invasive properties, as determined by in vitro assays. *Conclusion:* Our findings confirm the presence of two distinct subsets in the RCC52 line, and suggest the epithelioid subset being able to de-differentiate to clear cells, albeit partially, and harboring CSCs as an emerging therapeutic target in order to achieve effective treatment of this malignancy.

Sarcomatoid differentiation in renal cell carcinoma (RCC) is characterized mainly by a spindle-shaped mesenchymal cell histology (1). It is generally believed that sarcomatoid differentiation can arise from any of the RCC types, including clear cell, papillary, chromophobe, unclassified and collecting-duct carcinoma (2). The frequency of transformation is approximately 1-13% in RCC, depending on reports (3-6). Sarcomatoid RCC is well-known for its high incidence of metastases to the lung and bone at the first presentation (7). Patients who have primary and localized disease sarcomatoid RCC have 2-year and 5-year survival rates of only 25-40% and 14-22%, respectively (8, 9). Furthermore, patients with metastatic sarcomatoid RCC have a poor prognosis, with a medium overall survival of four to nine months from the time of diagnosis (7, 9-11).

Although it is well-known that sarcomatoid RCC can arise from any subtype of RCC, the detailed cellular and molecular events associated with tumor progression from clear cell RCC to sarcomatoid differentiation are largely unknown, as is the process of de-differentiation from sarcomatoid RCC to clear cell RCC, the latter being the most

Correspondence to: Dr. Shuen-Kuei Liao, Taipei Medical University, Taipei, Taiwan, R.O.C. E-mail: liaosk@h.tmu.edu.tw and Dr. Ming-Ling Kuo, Chang Gung University, Taoyuan, Taiwan, R.O.C. E-mail: mingling@mail.cgu.edu.tw

Key Words: Clear cell renal carcinoma, sarcomatoid differentiation, xenotransplantation, cell line and clonal sublines, de-differentiation, epithelioid, fibroblastoid.

prevalent among various RCC subtypes, at a frequency of about 75% (12, 13). We previously made an initial characterization of a sarcomatoid RCC cell line known as RCC52, and found that this cell line consisted of epithelioid and fibroblastoid subsets, both with total loss of human leukocyte antigen (HLA) class I expression caused by the co-existence of distinct mutations in the two encoding β_2 -microglobulin genes (14). To extend this study, we herein present our results of immunophenotyping of the RCC52 cell line and its clonal sublines derived thereof. An attempt was also made to evaluate the potential de-differentiation capability of sarcomatoid RCC cells to clear cells through xenotransplantation analysis of the RCC52 parental line and its clonal sublines in immunodeficient mice. To our surprise, de-differentiation of sarcomatoid RCC to clear cell RCC occurred *in vivo*, in spite of major structural defects of the genes leading to the total loss of HLA class I molecules demonstrated previously for RCC52 cells (14). We confirmed the co-existence of both epithelioid and fibroblastoid subsets in this cell line. Moreover, the epithelioid, but not fibroblastoid subset, of this sarcomatoid cell line was found to be tumorigenic in immunodeficient mice, showing its ability to de-differentiate, *albeit* partially, from a sarcomatoid to clear cell type *in vivo*.

Materials and Methods

Patient tumor specimens and tissue processing for cell culture. A 55-year-old male patient was admitted to Chang Gung Memorial Hospital, Taoyuan, Taiwan, with chief complaints of intermittent fever for two weeks and body weight loss of more than 10 kg in three months. Renal sonography found a 10-cm mass in the lower pole of the right kidney with heterogeneous echogenicity. Abdominal computed tomography and magnetic resonance arteriography showed a heterogeneous tumor mass suspicious for renal vein thrombosis and paracaval lymphadenopathy. Radical nephrectomy with lymph node dissection was performed and histopathology disclosed a Fuhrman's grade IV sarcomatoid RCC with capsular invasion. No renal vein thrombus was found but the dissected lymph nodes showed metastatic RCC. Bone scintigraphy was negative for bony metastasis. Immunotherapy with interferon was started. Unfortunately, recurrent disease in para-aortic and retroperitoneal lymph nodes were found six months later and lung metastasis was noted one year after nephrectomy. In spite of immunotherapy with interferon- α -2b (3 MIU/vial) given three times a week, pleural effusion developed and the patient's condition deteriorated. The patient died three months later, 18 months after the surgery.

Aside from routine pathology for diagnosis, a portion of the surgically-removed tumor tissue from the radical nephrectomy was sent to our research laboratory to be processed for cell culture and cryopreservation. The monodispersed cells were cultured as monolayers which have been maintained *in vitro* for over 50 passages. The original tumor was initially diagnosed histopathologically as sarcomatoid RCC, and after careful evaluation of the tumor sections, it was later found to be a mixture of both sarcomatoid and clear cell components, with the sarcomatoid

component being dominant. The cell line was designated RCC52 and was grossly of the mesenchymal cell morphology, suggesting that only cells of the sarcomatoid but not the clear cell element were adapted and maintained under our culture conditions (14). Clonal sublines were isolated from the RCC52 cell line at passage 37 *via* a limiting dilution method as described previously (14). For the sake of convenience, the designations E1–E6 were used to replace those epithelioid sublines originally known as E1A5, E3D4, E4D7, E4F5, E2G5 and E3D2, respectively, and the designations M1–M4 to replace those fibroblastoid sublines originally known as M1B4, M2D6, M1F7 and M1G7, respectively (14). The use and processing of the patient specimens was approved by the Institutional Review Board of Chang Gung Memorial Hospital, Taiwan (98-0535B) before the project started.

Growth curves. Cells were seeded at 1×10^5 cells/well in a 6-well plate (diameter of 3 cm; Nunc, Roskilde, Denmark) with 2 ml RPMI-1640 medium supplied with 10% heat-inactivated fetal bovine serum (FBS) at day 0. Cells were then detached from the bottom of wells at 24-h intervals for five days without change of medium, and by trypan blue exclusion assay, cells harvested at each time point were counted under a light microscope. Triplicate wells were used for each time point. The population doubling time and saturation density of cells were calculated from the growth curve. The supernatant from each well was collected and stored at -80°C until the quantification of transforming growth factor- β 1 (TGF- β 1) by enzyme-linked immunosorbent assay (ELISA).

Monoclonal antibodies and cytofluorometric analysis. A panel of monoclonal antibodies (mAbs) used for immunophenotyping including mAbs to Cytokeritin AE-1 (AE-1, clone AE-1; Signet, Dedham, MA, USA), AE-3 (clone AE-3; Signet), B-cell lymphoma 2 (BCL2, clone 124; Dako, Glostrup, Denmark), BH8.23 (S-K Liao), CD44s (clone DF1485; Dako), CD44v5 (clone VFF-8; Bender MedSystems, Burlingame, CA, USA), CD44v6 (clone VFF-7; Bender MedSystems), CD44v7 (clone VFF-9; Serotec, Oxford, UK), CD44v7-8 (clone VFF-17; Biosource, Camarillo, CA, USA), CD44v10 (clone VFF-14; Biosource), CD54 (clone M7063; Dako), CD58 (clone MEM-63; Serotec), CD105 (clone SN6h; Lifespan Biosciences, Seattle, WA, USA), E-Cadherin (clone 67A4; Biotec, Kennebunk, ME, USA), Epidermal growth factor receptor (EGFR, clone R-1; Santa Cruz Biotechnology, Santa Cruz, CA, USA), Lewis Y (Le^y, clone SDZ-ABL364; from Dr. H. Loibner, SANDOZ Research Institute, Vienna, Austria), Epithelial membrane antigen (EMA, clone E29; Dako), Epithelial cell adhesion molecule (EpCAM, clone 323/A3; Thermo Fisher Scientific, Fremont, CA, USA), HLA class I (clone W6/32; Thermo Fisher Scientific), HLA-DR (clone DK22; Dako), Heat shock proteins 70 (HSP70, clone C92F3A-5; Stressgen, Ann Arbor, MI, USA), N-Cadherin (clone 3B9; Zymed, South San Francisco, CA, USA), Proliferating cell nuclear antigen (PCNA, clone PC10; Dako), S100 (clone 15E2E2; Sigma, Saint Louis, MO, USA), S100- α (clone SH-A1; Sigma), S100- β (clone SH-B1; Sigma), S100-A4 (polyclonal; Abcam, Cambridge, MA, USA), URO-1 (clone J143; GeneTex, Inc., Irvine, CA, USA), URO-2 (clone S4; Covance, Berkeley, CA, USA), URO-4 (clone S27; GeneTex, Inc.), URO-5 (clone T16; Signet), URO-7 (clone S22; Signet), URO-8 (clone F31; Signet), URO-9 (clone Om5; Signet), URO-10 (clone T43; Signet), Vascular endothelial growth factor (VEGF, clone G153-694; BD Pharmingen, Franklin Lakes, NJ, USA) and

vimentin (clone V9; Dako). These were all aliquoted in small volumes and stored at -40°C . The aliquoted tubes containing mAbs were removed from the freezer, diluted to $5\ \mu\text{g/ml}$ or the concentration suggested by the manufacturer before use in cytofluorometric analysis, which was performed as previously described (14).

Cell migration and invasion assays. The *in vitro* cell invasion assay was performed using a BioCoat Matrigel (Becton Dickinson Biosciences, Bedford, MA, USA) and Transwell® Permeable Supports $8\ \mu\text{m}$ PolyCarbonate Membrane in a 24-well plate (Corning Life Sciences, Lowell, MA, USA). Matrigel was diluted with the serum free RPMI-1640 medium to $5\ \text{mg/ml}$ and added to the center to each cell well insert with a total volume $100\ \mu\text{l}$. Matrigel was then spread across the entire surface of the membrane, which was then allowed to stand for 1 h at 37°C . The cells were suspended in the RPMI-1640 medium containing 1% FBS and 1×10^5 cells seeded within $200\ \mu\text{l}$ medium in the upper chamber. The lower chamber contained complete culture medium supplied with 10% FBS. The duration of incubation time was 3, 6 and 9 h. The cell invasion ability was determined by counting cells in the lower chamber which had passed through Matrigel-coated membrane. The cell migration assay was performed by adding the cells directly without the coating process of Matrigel. The cells at the bottom of the membrane were fixed in methanol and stained by Giemsa stain. Cells in three randomly selected microscopic fields ($\times 400$ magnification) were then counted. Each experiment was repeated three times.

ELISA. The detection of TGF- $\beta 1$ in the spent media was performed using ELISA kits (R&D systems, Minneapolis, MN, USA) according to the manufacturer's instructions. The spent media of cultures were harvested at day 1, 3 and 5 after initiation of culture as in growth curve studies.

Anchorage-independent colony-formation assay. For the colony-formation assay, 6-well plates (Corning) were previously coated with 1% ultralow agarose (Sigma) in RPMI-1640 complete medium to avoid cells seeded adhering to the bottom. Each cell population was suspended at a density of 5,000 cells/ml/well in RPMI-1640 complete medium with 0.5% ultralow agarose and then plated on the top of a 1% ultra-low agarose basal layer ($n=3$) for each cell preparation. One microliter complete medium was added on top of the solidified layer to avoid loss of water by evaporation. After 28 days' culture at 37°C in a humidified atmosphere containing 5% CO_2 and 95% air, the colonies developed in agar were stained by crystal violet overnight, photographed, and then manually counted in the entire field of each well.

Protein extraction and western blot analysis. Cells were extracted with lysing buffer [RIPA buffer with 0.5 mM phenylmethylsulfonyl fluoride (PMSF), 0.1% protease inhibitor cocktail and 0.5 mM dithiothreitol (DTT)] and incubated on ice for 30 min. After centrifugation at $14,000 \times g$ for 30 min at 4°C the supernatant containing protein extracts was collected. For western blot analysis, $40\ \mu\text{g}$ of protein were subjected to 10% sodium dodecyl sulfate (SDS)-polyacrylamide gel electrophoresis. Following gel electrophoresis, the proteins were transferred to a polyvinylidene fluoride (PVDF) membrane (Immobilon P, Millipore, Bedford, MA, USA), which was then incubated with goat antibody to glucose-

regulated protein 78 (GRP78) (N-20; Santa Cruz Biotechnology), or mAb to β -actin (clone C4; Chemicon, International, Temecula, CA, USA). The membrane was then incubated with secondary antibodies, rabbit anti-goat or rabbit anti-mouse polyclonal antibodies, respectively, conjugated with horseradish peroxidase (HRP; Abcam). Following washing, the antigen-antibody complex on the membrane was detected by ECL western blotting detection reagents (Amersham Biosciences). Band intensities were quantified from scanned bands using Image J (National Institutes of Health, Bethesda, MD, USA), and results are expressed as fold-increases relative to those of the β -actin control.

Xenotransplantation in immunodeficient mice. Tumorigenicity assay was carried out in two different strains of immunodeficiency mice: nude and nonobese diabetic/severe combined immunodeficiency (NOD/SCID). The analyses were conducted upon approval from the Animal Ethics Committee, Chang Gung University, Taiwan. Six-week-old female nude mice (nu/nu) with the BALB/c background ($n=4$) were purchased from the National Laboratory Animal Center, Taipei. Six-week-old female NOD/SCID mice ($n=4$) were purchased from the National Taiwan University Hospital Animal Central facility, Taipei. Mono-dispersed cells were prepared from monolayer cultures of tumor cells by light trypsinization, followed by washing once in phosphate buffered saline (PBS). Cells (5×10^6 cells/0.1 ml PBS) were then injected subcutaneously at a site above the hind leg of each mouse. The animals were examined every two days for a period of 84 days to monitor the growth of tumors. The volume of palpable tumor nodules was calculated according to the formula: volume (mm^3)= $0.4 \times a \times b^2$, where a is the major diameter and b is the minor diameter perpendicular to the major one. At the end of observation period, animals were sacrificed and tumors were removed for either setting up cell culture and/or being fixed in Optimal Cutting Temperature compound (OCT) or in formaldehyde for immunohistology. All experiments were conducted in accordance with the Guide for the Care and Use of Laboratory Animals of the National Institute of Health and following the Institutional Animal Care and Use Committee (IACUC) protocol authorized by Chang Gung Memorial Hospital, Taiwan (CGU11-093).

Immunohistochemistry and immunocytochemistry. Sections ($5\text{-}\mu\text{m}$ in thickness) of formalin-fixed, paraffin-embedded RCC52 tumor blocks obtained from the mice xenografts were processed. Prior to immunostaining, the de-paraffinized slides were subjected to an antigen retrieval process by dipping the slides in a beaker containing 0.01 M sodium citrate (pH 6.0) in a boiling state on a hotplate. Following a 20 min incubation, the beaker was removed from the hotplate and allow to cool down at room temperature for 20 min. Slides were washed once in PBS and stained using the UltraVision Quanto Detection System HRP DAB kit (Lab Vision Corporation, Fremont, CA, USA), according to the manufacturer's instructions. Antibody to HLA class I (clone W6/32), heavy chain (clone HC-10), β_2 -microglobulin ($\beta_2\text{m}$) (clone L368) and PAX2 (polyclonal; Invitrogen, Carlsbad, CA, USA) were used in this study. The W6/32 mAb specific for a nonpolymorphic determinant of the heavy chains associated with $\beta_2\text{m}$ was purchased from PharMingen, and mAbs HC-10 and L368 were generous gifts from Dr. Soldano Ferrone, Cancer Institute, University of Pittsburg, Pittsburg, PA, USA. For frozen sections and immunohistological staining, protocols followed were essentially those previously described (15).

Statistical analysis. All experiments were performed in triplicates or greater. Data are presented as the mean±SD of the indicated number of independent experiments. Student's *t*-test was employed to evaluate the results. Differences were considered statistically significant with *p*-values of less than 0.05.

Results

Establishment of the RCC52 cell line. The original patient's tumor appeared to be mostly of typical mesenchymal/sarcomatoid histopathology with occasional clear cell components in the lesion (Figure 1A and B). This suggests that sarcomatoid cells in this sarcomatoid tumor lesion must have been transformed or differentiated from clear cell RCC at the primary site. When monodispersed cells prepared mechanically from the tumor specimen were cultured in complete medium in two dishes, most cells settled and attached to the bottom of the dishes after overnight incubation. They started to grow and formed monolayers rather quickly during the first two days, reaching confluence at day 5 and day 6. These cells were sub-cultured to new culture vessels containing fresh complete medium and expanded *in vitro* rather efficiently. When grown as monolayers, the cells consisted mostly of epithelioid cells with a minority of small-sized spindle/fibroblastoid cells (Figure 1C). We used these cells at passages between 25 and 35 for subsequent analyses.

Live cells of monolayer cultures from E1–E4 and those from M1–M4 are illustrated in Figure 1D. A higher frequency of scattered reflective round cells was clearly noted for each of the four epithelioid sublines as compared with each of the four fibroblastoid sublines in which only fibroblastoid cells were evident.

In vitro growth characteristics of parental and clonal sublines of the RCC52 cell line. In order to characterize the growth pattern of RCC52 cells, growth curves were constructed in two separate experiments. These two experiments yielded almost identical results (Figure 1E and F). Based on this growth curve, the population doubling time was about 23.4 h and the saturation density was 5.5×10^4 cells/cm². Of note is that cell viability was maintained up to 90% during the exponential phase, and once confluence was reached at about day 3, monolayer cells started to detach from the bottom of culture vessels.

We also investigated the *in vitro* growth differences between four epithelioid and four fibroblastoid clonal sublines (Figure 1E and F). The growth curve data revealed that the epithelioid sublines grew much faster than the fibroblastoid ones (doubling time: 32.0 ± 4.3 vs. 50.1 ± 2.8 h) and reached a higher saturation density (5.5 ± 0.6 vs. $3.5 \pm 0.7 \times 10^4$ cells/cm²) (Figure 1E). In association with these features, all the epithelioid sublines exhibited two additional characteristics, namely density sensitivity and rapid decline in cell viability once the cells reached the growth plateau, while all the fibroblastoid sublines maintained most of their

Table I. Expression of selected surface and cytoplasmic markers by RCC52 cells as determined by cytofluorometric analysis.

Marker	% Positive cells (MFI)	
	Surface	Cytoplasm
HLA class I	–	–
AE-1	ND	81.8 (102.3)
AE-3	ND	13.8 (14.6)
HSP70	–	75.2 (25.6)
BH8.23 (50-55 kDa)	–	93.6 (66.7)
EMA	–	–
CD44s	98.4 (154.6)	99.6 (92.0)
CD44v5	–	80.7 (26.1)
CD44v6	–	99.2 (68.4)
CD44v7	14.2 (509.6)	99.6 (139.8)
CD44v7-8	–	99.3 (93.3)
CD44v10	–	–
CD54	22.2 (80.7)	ND
CD58	84.7 (32.2)	ND
Le ^y	–	–
BCL2	ND	20.2 (18.9)
EpCAM	–	–
E-Cadherin	10.8 (28.1)	–
N-Cadherin	–	81.2 (21.1)
EGFR	98.7 (78.9)	ND
HLA-DR, -DP, -DQ	–	ND
Vimentin	ND	99.8 (206.8)
S100	ND	98.8 (39.4)
S100-α	ND	–
S100-β	ND	88.1 (41.7)
S100-A4	ND	52.7 (18.1)
VEGF	ND	98.3(30.7)
URO-1	99.1 (140.6)	99.9 (220.0)
URO-2	–	10.3 (16.2)
URO-4	–	–
URO-5	–	28.0 (15.8)
URO-7	–	–
URO-8	–	–
URO-9	–	17.7 (14.8)
URO-10	99.4 (203.2)	18.2 (19.4)
NMIg	–	–

MFI, Mean fluorescence intensity in arbitrary units; –, signifies a negative result, with % positive <10%; ND, not done; AE-1, cytokeritin AE-1; HLA class I, human leukocyte antigen class I; HSP70, heat shock proteins 70; EMA, epithelial membrane antigen; Le^y, Lewis Y; BCL2, B-cell lymphoma 2; EpCAM, epithelial cell adhesion molecule; EGFR, epidermal growth factor receptor; VEGF, vascular endothelial growth factor; NMIg, normal mouse immunoglobulin.

typical adherent cell morphology on the culture substrates, with a higher percentage of viability throughout the five days of culture (Figure 1F).

Immunophenotyping of parental and clonal sublines of the RCC52 cell line. Various mAbs were used to characterize the RCC52 cells by indirect immunofluorescence/flow cytometric analysis (Table I). Consistent with our previous observations

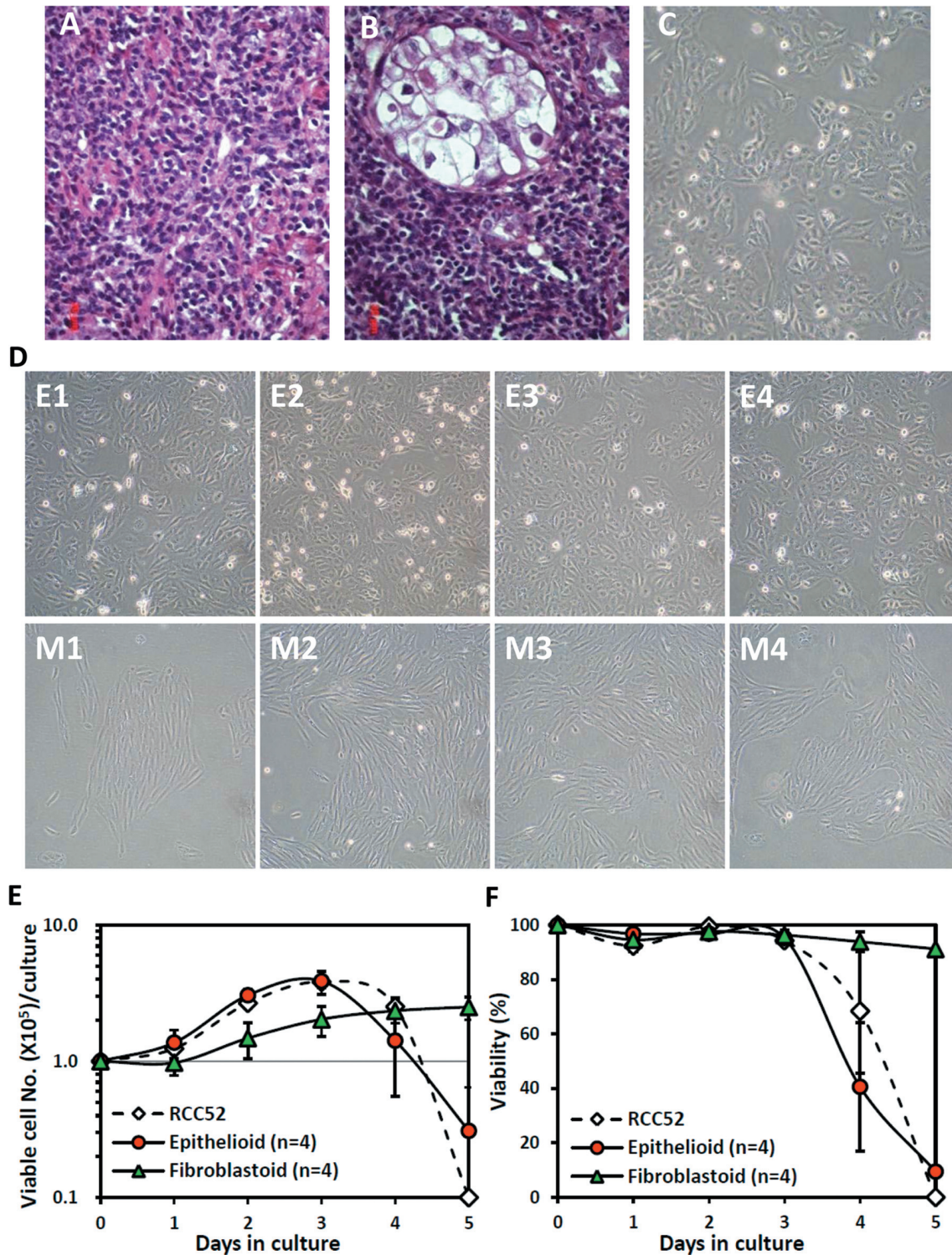


Figure 1. Histopathology of tumor and in vitro growth of RCC52 parental and fibroblastoid clonal sublines. A, B: Histopathology (H&E staining) of the original tumor lesion from which the RCC52 cell line originated. In A, the typical sarcomatoid renal cell carcinoma (RCC) histology with spindle-shaped pleomorphic cells can be seen, while in B, clear cell components are clearly separated from the sarcomatoid component. Original magnification, $\times 400$. C: Live monolayer culture of RCC52 cells established from the original patient tumor. Original magnification, $\times 100$. D: Live monolayer cultures of epithelioid (E1–E4) and fibroblastoid sublines (M1–M4). Original magnification, $\times 100$. E, F: Growth curves of the RCC52 parental cells, epithelioid and fibroblastoid sublines cultured in vitro in which the total viable cell number/dish and percentage cell viability at each time point are indicated. Each time point represents the mean \pm SD of triplicate wells.

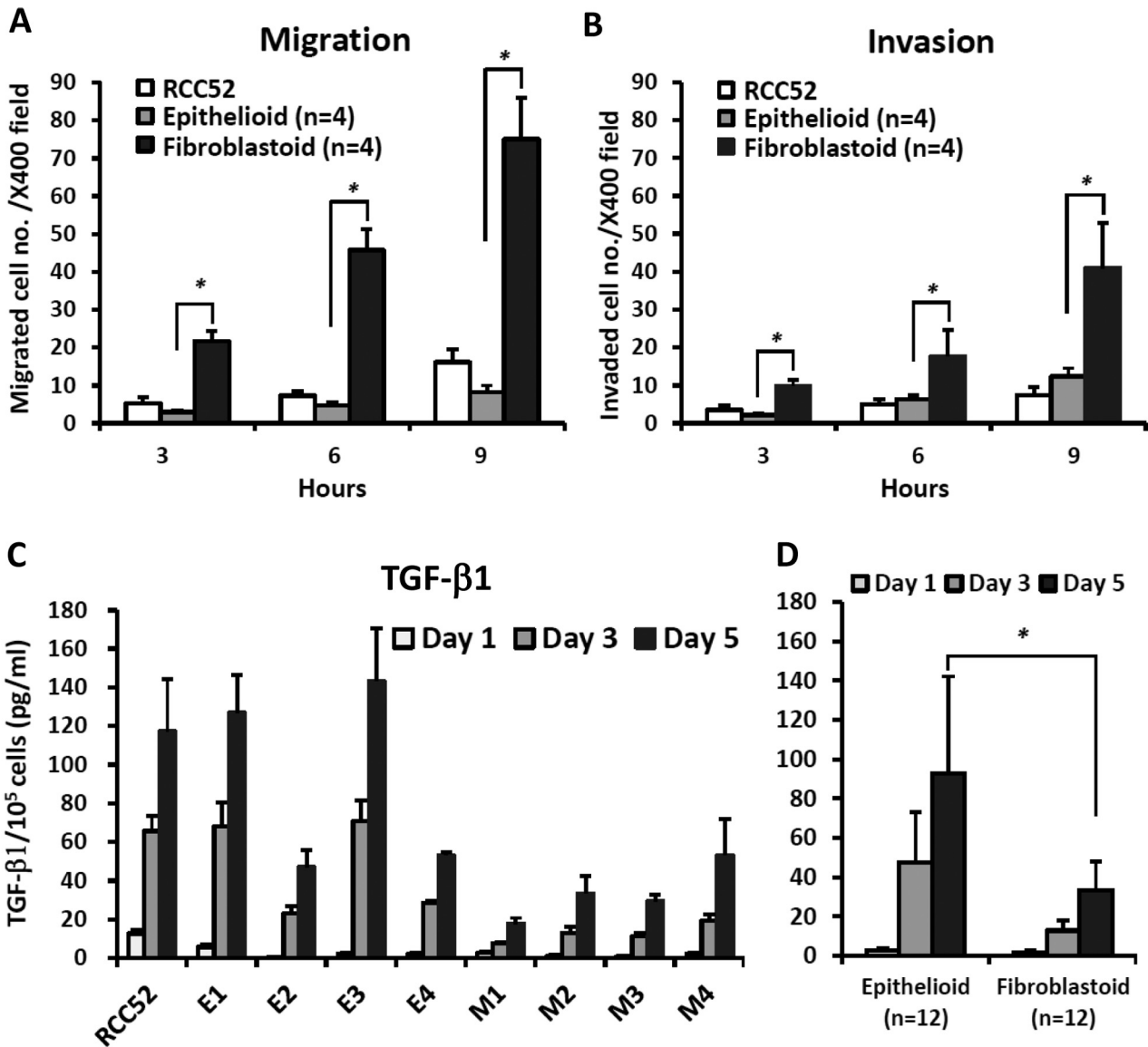


Figure 2. *In vitro* migration/invasion potential and transforming growth factor-β1 (TGF-β1) secretion levels of two types of RCC52 clonal sublines. Migration (A) and invasion (B) potential of epithelioid (E1–E4) vs. fibroblastoid sublines (M1–M4). Cell migration and invasion assays were conducted in a modified 24-well Boyden chamber with a membrane without coating and coated with Matrigel, respectively. A total of 1×10^5 cells were suspended in the RPMI-1640 medium containing 1% fetal bovine serum (FBS) and seeded in the upper chamber. The lower chamber contained of complete culture medium with 10% FBS as chemotactic stimulus. After incubation for 3, 6 and 9 h, the migrated and invaded cells were fixed in methanol and stained by Giemsa. Cells in three randomly selected microscopic fields ($\times 400$ magnification) were counted. The number of cells at every time point was determined in triplicate and results are expressed as the mean \pm SD. C: The supernatants collected in growth curve studies at days 1, 3 and 5 were assayed for TGF-β1 by ELISA. D: The mean concentrations of TGF-β1 secreted by the two different subsets at days 1, 3 and 5 (where levels at each time point were determined in triplicate wells, $n=12$) were compared and analyzed. The difference in TGF-β1 secretion between these two cell subsets at day 5 was found to be significant. * $p < 0.01$.

(14), HLA class I expression was not detected on the cell surface nor in the cytoplasm of RCC52 cells. Selected epithelial markers, including cytoplasmic AE-1 and BH8.23 (50-55 kDa), were detected, while other epithelial markers, such as EMA, EpCAM and Le^y, were not detected. However, cytoplasmic N-

Cadherin, S100 and S100-β were abundantly expressed by RCC52 cells. When 10 markers of the URO series were examined, surface expression of URO-1 and URO-10 was high, whereas the corresponding cytoplasmic UROs were not consistently expressed. Of interest is that two mesenchymal

Table II. Surface and cytoplasmic expression of selected antigens by the RCC52 parental and clonal sublines as determined by cytofluorometric analysis.

Antigen	% Positive cells (MFI)									
	Parental		Epithelioid (E)				Fibroblastoid (M)			
	RCC52	E1	E2	E3	E4	M1	M2	M3	M4	
Surface										
HLA class I	-	-	-	-	-	-	-	-	-	
E-Cadherin	10.8 (28.1)	38.6 (18.2)	36.3 (28.4)	40.3 (19.0)	21.5 (22.8)	-	-	-	-	
N-Cadherin	-	-	-	-	-	-	-	-	-	
EpCAM	-	-	-	-	-	-	-	-	-	
EGFR	98.7 (78.8)	97.9 (53.4)	99.7 (54.9)	99.2 (70.8)	99.5 (172.3)	99.9 (112.6)	97.2 (92.3)	99.6 (146.3)	98.6 (89.7)	
NMIg	-	-	-	-	-	-	-	-	-	
Cytoplasmic										
HLA class I	-	-	-	-	-	-	-	-	-	
HSP70	78.0 (64.8)	97.6 (51.5)	97.4 (96.8)	98.7 (136.9)	99.2 (52.4)	13.6 (28.3)	33.8 (27.8)	47.5 (27.4)	58.5 (17.7)	
EMA	-	-	-	-	-	41.0 (16.2)	13.5 (22.4)	30.0 (10.8)	64.6 (17.5)	
BCL2	-	-	-	12.9 (44.9)	59.2 (16.2)	46.3 (13.9)	46.9 (21.3)	80.4 (13.2)	59.6 (13.8)	
E-Cadherin	-	-	-	-	-	-	-	-	-	
N-Cadherin	27.9 (15.6)	40.2 (15.4)	61.3 (17.0)	93.4 (21.8)	83.8 (14.6)	82.3 (21.5)	87.4 (14.4)	96.1 (23.4)	95.8 (39.9)	
S100-A4	52.7 (18.1)	88.9 (20.8)	70.0 (6.2)	65.4 (19.5)	60.9 (13.8)	82.3 (11.1)	48.2 (20.1)	82.3 (11.1)	35.1 (14.8)	
PCNA	99.0 (66.4)	98.5 (43.5)	97.8 (64.3)	99.0 (75.5)	99.6 (55.6)	99.0 (41.0)	97.1 (40.5)	96.4 (39.2)	99.4 (42.6)	
Vimentin	99.2 (630.8)	92.3 (349.2)	95.6 (398.7)	99.7 (342.2)	99.3 (196.0)	99.5 (311.2)	98.9 (365.9)	99.3 (307.8)	98.8 (270.0)	
NMIg	-	-	-	-	-	-	-	-	-	

MFI, Mean fluorescence intensity in arbitrary units; -, signifies a negative result, with % positive <10%; HLA class I, human leukocyte antigen class I; EpCAM, epithelial cell adhesion molecule; EGFR, epidermal growth factor receptor; NMIg, normal mouse immunoglobulin; HSP70, heat shock proteins 70; EMA, epithelial membrane antigen; BCL2, B-cell lymphoma 2; PCNA, proliferating cell nuclear antigen.

markers, vimentin and N-Cadherin, were strongly expressed in the cytoplasm. Furthermore, surface EGFR and cytoplasmic VEGF were expressed abundantly. S100-A4 was found in 53% of RCC52 cells. Two intercellular adhesion molecules (CD54 and CD58), which are considered to be important in mediating non-major histocompatibility complex (MHC) restricted natural killer (NK)/lymphokine-activated killer cell (LAK) cytotoxicity (16, 17), were found to be expressed adequately by RCC52 cells (22.2 and 84.7%, respectively).

Differences between the epithelioid and fibroblastoid sublines were further compared by cytofluorometric analysis. Results revealed clear differences between these two morphologically-distinct cell subsets (Table II). Moderate levels of surface E-Cadherin were detected in all four of the epithelioid, but not in all of the fibroblastoid sublines tested. On the other hand, moderate levels of cytoplasmic EMA and BCL2 were detected only in the fibroblastoid, but not epithelioid, sublines, with one exception, which was the E4 subline. At variance from other epithelioid sublines, E4 expressed a significant level of BCL2 positive cells (59.2%), which was in fact comparable to those expressed by fibroblastoid sublines (58.3±16.0%). The cytoplasmic HSP70 was expressed at higher levels by the epithelioid sublines

(98.2±0.87) in terms of percentage positive cells, as compared with those by the fibroblastoid ones (38.4±19.3). The difference is statistically significant ($p<0.01$). No consistent differences in the cytoplasmic expression of S100-A4, PCNA, or vimentin were found between the two types of sublines.

Difference in cell migration and invasion ability between the epithelioid and fibroblastoid clonal sublines. In order to determine the migration and invasion ability of the RCC52 epithelioid and fibroblastoid sublines, we used transwells with a pore size of 8 μ m coated without and with Matrigel, in order to perform these two experiments independently. We chose three time points, 3, 6 and 9 h, to calculate the migrated and invaded cell numbers respectively. As shown in Figure 2A and B, both the numbers of migrated and invaded cells in the fibroblastoid sublines were much higher than those in the epithelioid sublines at the three time points tested ($p<0.01$).

Differential release of TGF- β 1 by epithelioid and fibroblastoid subsets. The four epithelioid sublines tested secreted appreciable amounts of TGF- β 1 (47-143 pg/10⁵ cells) in the spent medium over a period of five days,

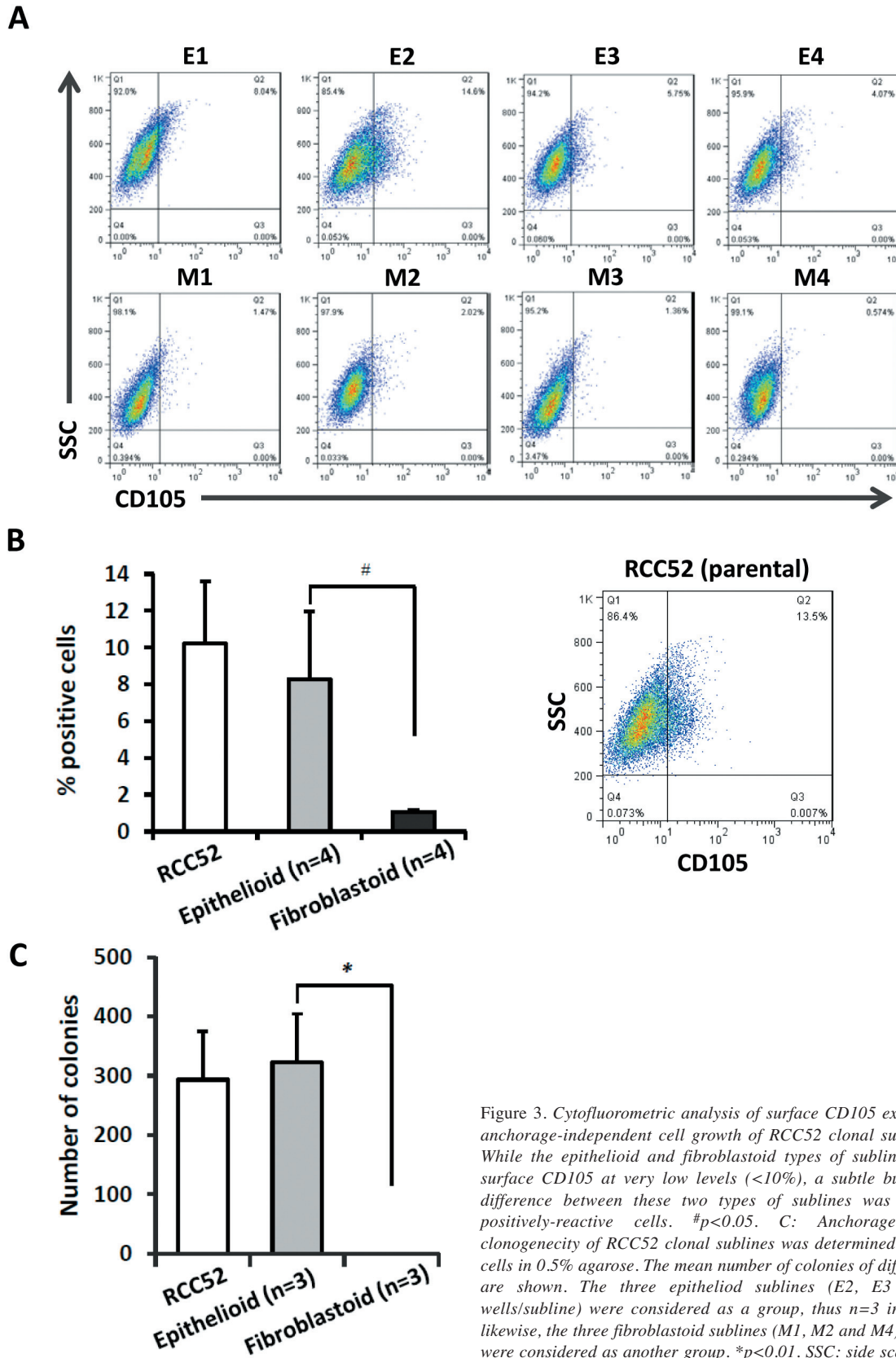


Figure 3. Cytofluorometric analysis of surface CD105 expression and anchorage-independent cell growth of RCC52 clonal sublines. A, B: While the epithelioid and fibroblastoid types of sublines expressed surface CD105 at very low levels (<10%), a subtle but significant difference between these two types of sublines was revealed by positively-reactive cells. # $p < 0.05$. C: Anchorage-independent clonogenicity of RCC52 clonal sublines was determined by culturing cells in 0.5% agarose. The mean number of colonies of different groups are shown. The three epithelioid sublines (E2, E3 and E4, 3 wells/subline) were considered as a group, thus $n = 3$ in this group; likewise, the three fibroblastoid sublines (M1, M2 and M4), where $n = 3$, were considered as another group. * $p < 0.01$. SSC: side scatter.

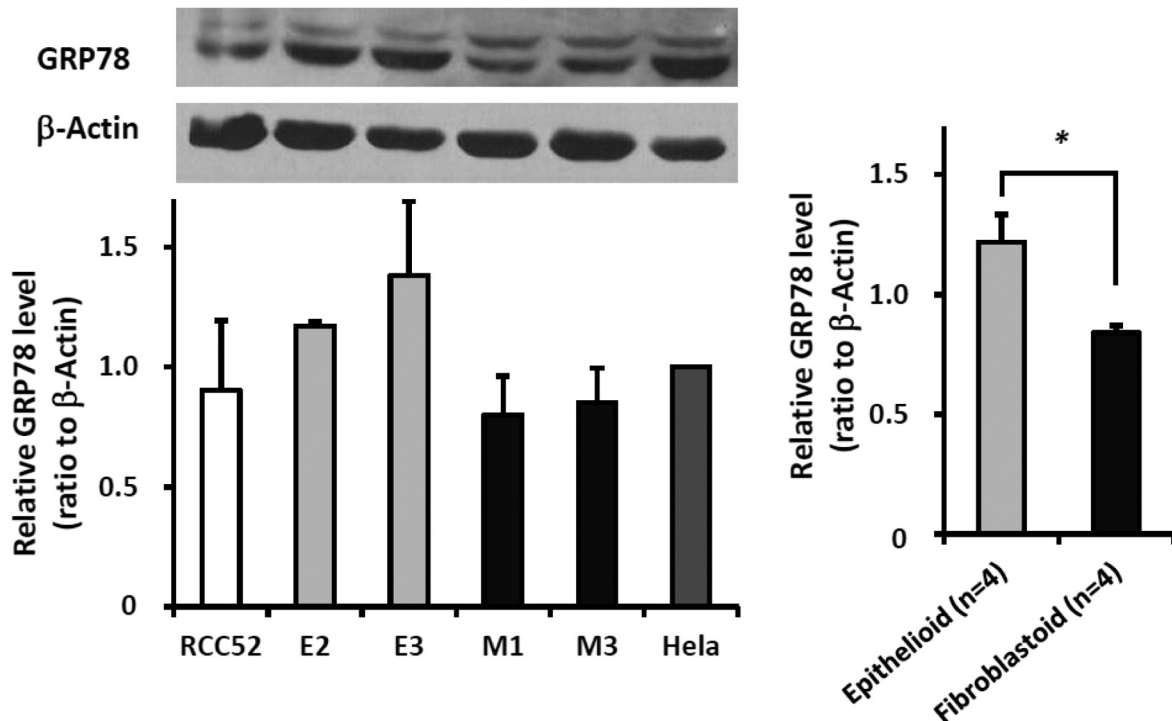


Figure 4. Western blot of GRP78 in RCC52 clonal sublines. Western blot analysis of the expression of GRP78 in epithelioid (E2 and E3 as representatives) vs. fibroblastoid (M1 and M3 as the representatives) clonal sublines. The HeLa cell line served as a positive control. Data were obtained by normalizing levels of GRP78 to those of β -actin from three independent experiments with four epithelioid and four fibroblastoid sublines. Results are expressed as the mean \pm SD. * p <0.01.

whereas the four fibroblastoid sublines tested secreted lower levels of TGF- β 1 (17.6–53.2 pg/10⁵ cells) in culture, both in a time-dependent manner (Figure 2C). The difference in TGF- β 1 release from these two subsets of cells at day 5 was compared and found statistically significant (Figure 2D).

Difference in CD105 expression between epithelioid and fibroblastoid clonal sublines. The marker CD105 has been shown to be a marker of cancer stem cells (CSC) or tumor-initiating cells of RCC (18). Cytofluorometric analysis indicated that while both types of sublines, like the parental RCC52 cells, exhibited fewer than 10% of cells with positive reactivity, in three repeated experiments, the epithelioid sublines invariably exhibited a higher percentage of positive stained cells as compared with the fibroblastoid ones (8.29 \pm 3.66% vs. 1.05 \pm 0.08%; p =0.034) (Figure 3B). The results of a representative experiment are depicted in Figure 3A.

Anchorage-independent colony-forming ability of parental RCC52, epithelioid and fibroblastoid sublines. We used a soft agar colony-formation assay to compare the anchorage-independent growth ability of parental RCC52 cells, epithelioid and fibroblastoid sublines. The results show that both the parental RCC52 cells and epithelioid sublines gave

rise to colonies, and the colony number was higher in parental RCC52 cells than that in the epithelioid sublines, while in the fibroblastoid sublines tested, essentially no colonies were developed (Figure 3C).

Difference in GRP78 expression between the epithelioid and fibroblastoid clonal sublines. GRP78 protein, a stress-related heat-shock protein, is known to play an important role in regulating different malignant phenotypes, including cell growth, migration and invasion (19, 20). Differential expression of GRP78 at the protein level was determined among representative epithelioid and fibroblastoid sublines, as well as in the parental RCC52 cell line (Figure 4). Greater amounts of GRP78 were expressed by the epithelioid sublines as compared with the fibroblastoid ones (p <0.01).

Xenotransplantability in immunodeficient mice and characterization of cell cultures re-established from the xenografts. RCC52 cells (5 \times 10⁶) were subcutaneously inoculated into each of four nude and four NOD/SCID mice. The development of solid tumors at the injection sites of the animal was carefully examined. All four nude mice injected with RCC52 cells developed solid tumors at the injection sites, with a mean tumor volume of 863.3 \pm 507.7 mm³ at day

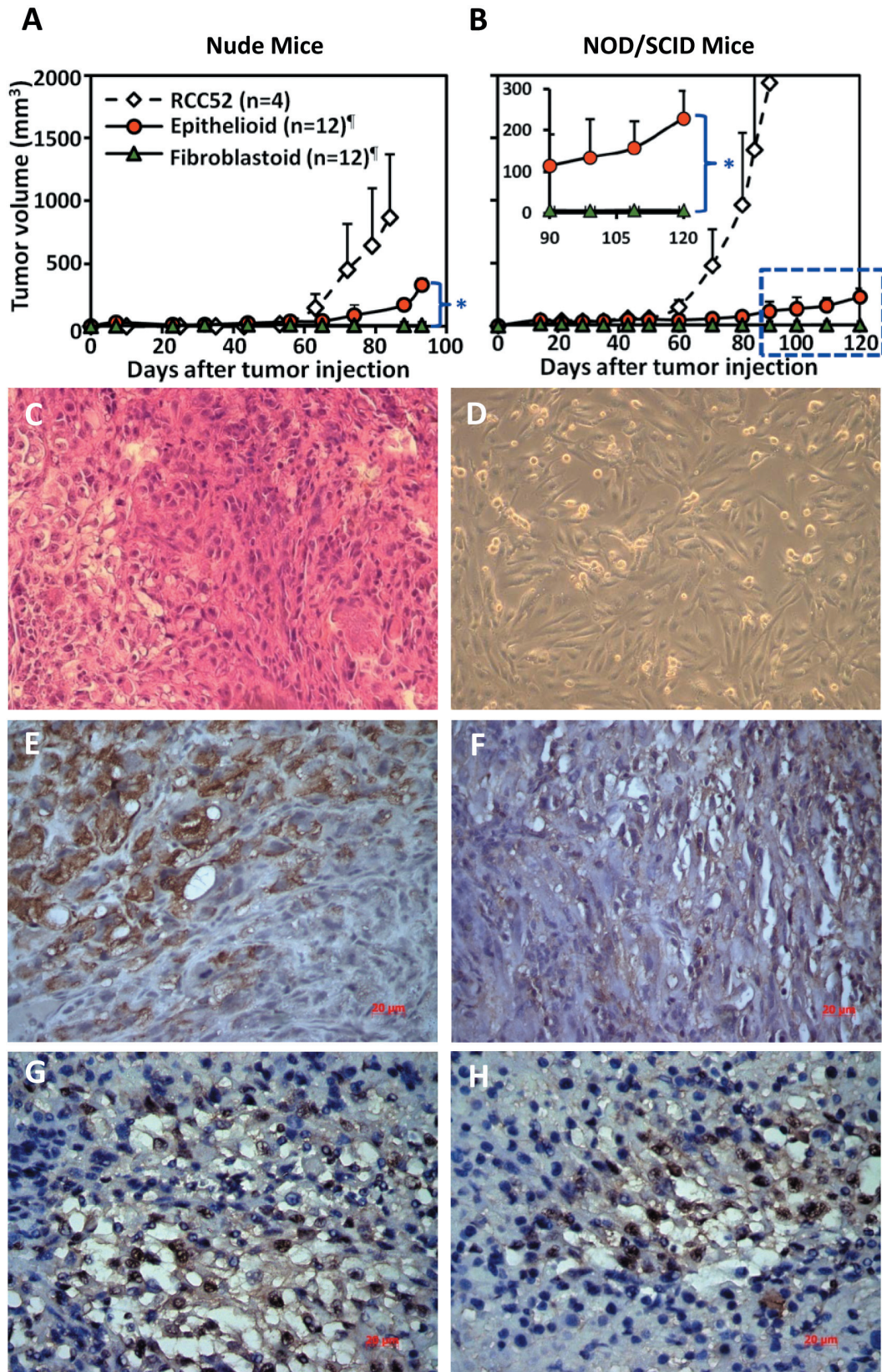


Figure 5.

84 following tumor cell injection (Figure 5A). There was an average latent period of approximately 45 days before the tumor started to increase in size. All four NOD/SCID mice injected with RCC52 cells also developed solid tumors, with a mean tumor volume of $1406.2 \pm 766.9 \text{ mm}^3$ at day 85 following tumor cell injection (Figure 5B). H&E staining of the tumor sections from the xenografts showed that the majority of tumor cells were of sarcomatoid histology, while surprisingly, only small and focal areas exhibited clear cell morphology in the same tumor section (Figure 5C). The clear cell areas were invariably found to be nuclear-positive for PAX2 (Figure 5E), which is a transcription factor considered a marker for distinguishing clear cell RCC from sarcomatoid RCC (21-23). Cultured cells re-established from the NOD/SCID xenografts appeared similar in *in vitro* cellular morphology (Figure 5D) to the original RCC52 cells before they were subjected to xenotransplantation (Figure 1C). Consistent with the initially established RCC52 cell lines from the patient's biopsy material, no clear cells or PAX2⁺ cells could be detected on the *in vitro* re-established cultured monolayer sarcomatoid cells from the xenograft.

In xenotransplantation with the RCC52 clonal sublines, only epithelioid sublines developed tumors at the injection sites in both nude and NOD/SCID mice, whereas no tumor takes were observed in any of the three injected fibroblastoid sublines (Figure 5A and B). The average volumes of tumors generated by epithelioid sublines at the injection sites were found to be $329.6 \pm 57.0 \text{ mm}^3$ in nude mice at day 93 following tumor cell injection, and $229.6 \pm 66.7 \text{ mm}^3$ in NOD/SCID mice at day 120 following tumor cell injection. We also noted that the *in vivo* growth of the parental RCC52

cells was far more faster in terms of the mean growth rates and was much greater than that of the epithelioid sublines in terms of the tumor volume.

Immunohistochemistry of xenografts resulting from subcutaneous injection of parental and clonal sublines of the RCC52 cell line. Immunohistochemistry conducted on cryosections of OCT-embedded RCC52 xenografts removed from nude mice showed that the tumor cells were negative for HLA class I when tested with W6/32 mAb to HLA class I or L368 mAb to $\beta_2\text{m}$. The negative reactivity of these mAbs was also found with for clear cell component in the sarcomatoid component of the same xenograft tissue section. Immunoreactivity with the HLA class I heavy chain-specific mAb HC-10 resulted in moderate staining of the clear cell component, and in weak staining of the sarcomatoid component of the malignant tumor (results not shown). However, no reactivity of the xenografts developed from nude or NOD/SCID mice were found for both HLA class I and $\beta_2\text{m}$, in contrast to the reactivity of the original tumor removed surgically, in which the sarcomatoid component was HLA class I-negative, whereas clear cell components exhibited HLA class I- and $\beta_2\text{m}$ -positivity (14). Another important marker, PAX2 was found to be expressed in the nuclei with a high frequency in most RCC tumor types, including renal cell adenocarcinoma (data not shown), but not in sarcomatoid RCC (21). Here, we used this PAX2 marker to verify the clear cell components in the nude or NOD/SCID mouse xenografts. Immunostaining with anti-PAX2 on tissue sections of RCC52 xenografts showed positive reactivity with the clear cell component/area, but negative with the sarcomatoid component (Figure 5E). When the sections of xenografts resulting from the injection of epithelioid sublines were tested immunohistochemically, clear cell areas were occasionally found and invariably stained positively for PAX2, while the sarcomatoid cell areas of the lesion were consistently PAX2-negative (Figure 5F). The results in Figure 5D (live cell culture), E and F (immunostained sections) just described were from or of nude xenografts. Very similar results were also obtained with xenografts developed in NOD/SCID mice. These results confirmed the presence of clear RCC cells in the xenograft as a result of subcutaneous inoculation of parental sarcomatoid RCC52 cells or the epithelioid sublines. In fact, similar patterns of reactivity were found for the original patient's formalin-fixed, paraffin-embedded tumor sections by immunohistochemistry, following an antigen retrieval process (Figure 5G and H).

Discussion

In this study, we documented the *in vitro* growth pattern, xenotransplantability and immunophenotyping profiles of the RCC52 cell line and the clonal sublines derived thereof. The two morphologically-distinct subpopulations in this cell line

←

Figure 5. Xenotransplantation of RCC52 parental and clonal sublines. Cells ($5 \times 10^6/0.1 \text{ ml PBS}$) of representative epithelioid (E2, E3 and E4) and fibroblastoid (M1, M2 and M3) sublines were injected subcutaneously in nude (A) and non-obese diabetic/severe combined immunodeficiency (NOD/SCID) (B) mice at the hind leg. The animals were examined for the growth of tumors every two days for a period of 84 days. The mean curves with standard deviations are also illustrated at each time point as dotted lines. ¶Note that three epithelioid and three fibroblastoid sublines were used in the experiments and four animals were used for subcutaneous injection of each subline, resulting in $n=12$ for each type of subline in analysis. * $p < 0.01$. C: Histopathology (H&E staining) of a xenograft in a nude mouse resulting from s.c. injection of 5×10^6 RCC52 cells/site is shown. Original magnification, $\times 400$. One area of clear cells was noted on the left side of the micrograph. D: Live culture of RCC52 monolayer cells established from the xenograft. Original magnification, $\times 100$. Immunostaining profiles for PAX2 positivity on the sections of a representative RCC52 xenograft (E), an epithelioid subline E3 xenograft (F) and of the original patient's tumor (G, H) are shown. Original magnification, $\times 400$. Note that positive nuclear staining for PAX2 was detected only in the clear cell areas among the sea of sarcomatoid components.

(epithelioid vs. fibroblastoid) were identified for the first time in a sarcomatoid RCC by our group (14) and further confirmed in this study. The ability of RCC52 cells to grow as solid tumors at the injection sites in nude, as well as NOD/SCID immunodeficient mice suggests the malignant potential of this cell line. One of the important findings of this study is that injection in immunodeficient mice with exclusively sarcomatoid RCC cells resulted in solid tumors of small independent areas of clear cell RCC in the sea of sarcomatoid tumor cells. This implies the high plasticity and malignant nature of sarcomatoid RCC cells. The clear cell and sarcomatoid cell components of the xenografts were both found to be β_2m -negative, in contrast to the patient's original tumor specimen in which the clear cell component was β_2m -positive while the sarcomatoid cell component was β_2m -negative (14). This indirectly proves that the clear cell component formed in the immunodeficient animals was indeed derived from the sarcomatoid RCC cells established as a cell-line in culture. We believe that our finding of sarcomatoid RCC52 cells to be able to de-differentiate into PAX2⁺ clear cells, *albeit* partially, is the first being reported, and that such de-differentiation was independent of major HLA class I structural defects, such as that in the β_2m gene. The structural defects include distinct mutations in the β_2m -encoding genes and loss of heterozygosity (LOH) in chromosome 15, as demonstrated previously (14). These defects did not seem to impede the ability of sarcomatoid RCC cells to de-differentiate into clear RCC ones in the RCC52 sarcomatoid cell line. Xenotransplantation analysis of the various clonal sublines de-differentiates into a clear cell type, further substantiates the notion of the occurrence of such de-differentiation. This may underscore the importance of the epithelioid subpopulation harboring the CSCs of this malignancy.

Earlier published articles in literature indicated more than 50% sarcomatoid RCCs examined as being positive for AE-1/AE-3, EMA and vimentin (24-27). Our current results showed that certain epithelial markers, such as AE-1 and BH8.23 (50-55 kDa), were expressed in the cytoplasm of RCC52 cells, while other epithelial markers, including EMA, Le^y and EpCAM, were not detected on the cell surface or in the cytoplasm. However, surface expression of E-Cadherin was detected. The two mesenchymal markers, vimentin (99.8%) and N-Cadherin (81.2%), were invariably expressed in the cytoplasm of RCC52 cells. One of the most unusual findings was that EMA was detected in the cytoplasm of all four fibroblastoid sublines but none of the epithelioid sublines maintained independently in culture for few passages, and was not detected in the parental RCC52 cells. This could be due to the possibility that cell-cell contact or mediators released from the epithelioid subset in the parental line may have affected fibroblastoid expression of EMA. We have not yet tested this possibility. As yet, none of the surface markers identified thus far are useful for effective isolation of these two subsets of RCC52 cells.

Reduced E-Cadherin expression in sarcomatoid RCC was thought to be associated with tumor trans-differentiation (28). Loss of E-Cadherin and gain of N-Cadherin are the hallmarks of the epithelial-to-mesenchymal transition (EMT), regarded as a critical event in morphogenetic change during cancer progression (29, 30). S100-A4 has been considered a marker of tumor progression and metastasis (31), as well as a common mediator of EMT (32). In the current study, RCC52 cells were positive for surface expression of E-Cadherin (10%) and negative for surface expression of N-Cadherin (2.18%). On the other hand, RCC52 cells were positive for cytoplasmic N-Cadherin, vimentin and S100-A4. Of the two morphologically-distinct subpopulations, only the epithelioid one was positive for surface expression of E-Cadherin (21.5-40.3%). In repeated experiments, we noted that E4, one of the four epithelioid sublines, consistently exhibited a considerably high BCL2-positive reactivity which was similar to the four fibroblastoid sublines (Table II). The reason for E4 to be distinct itself from the other three epithelioid sublines in this regard is not immediately clear, and merits further investigation. It should be pointed out that it is not easy to distinguish epithelioid cells from fibroblastoid cells on RCC52 monolayer cultures or on H&E stained slides of the lesion.

It has been demonstrated that molecular cross-signaling between cancer cells and stromal fibroblasts might stimulate migration of both cell types towards each other and modify the adjacent extracellular matrix (ECM) and basement membrane, resulting in the breakdown of normal tissue basement membranes (33). TGF- β , a chemotactic agent for fibroblasts (34), is implicated in the signaling from the epithelioid component to the fibroblastic component of a tumor. Of note is that the fibroblastoid subset in our study was believed to have progressively evolved with genetic changes during primary tumor development and progression, along with the clear cell RCC cells to sarcomatoid differentiation. In other words, this may be the mechanism by which tumorigenic epithelioid cells contribute to the coordination of invasion of the tumor-associated non-tumorigenic fibroblastoid cells in the sarcomatoid RCC52 cell line/tumor. This process is likely carried out *via* the regulation of 'epithelioid' cancer-derived TGF- β . We believe that this interactive cross-signaling between these two cell subsets influences the invasive behavior of both cell populations, leading to concerted invasion of this tumor to lymph nodes in the patient from which the RCC52 cell line was derived. Our observations that tumorigenicity and migratory/invasive properties can be clearly dissociated and independently ascribed to the two subsets of RCC52 cells are quite different from those exhibited by other tumor systems. In the latter, a cell entity responsible for tumorigenicity was also closely associated with greater migratory/invasive potential, *i.e.* by the same cell type harboring CSCs playing

two diverse functions. Examples of such cases include squamous cell carcinoma (35), gastrointestinal cancer (36), and prostate cancer (37).

The slower growth rate and smaller tumor size of xenografts developed by the epithelioid sublines as compared with those developed by parental RCC52 cells may be due to the clonal sublines that we isolated not being the tumor variants harboring the major classes of CSCs in this line/tumor. Such a contrast may also be due to the highly artificial situation created by separating epithelioid and fibroblastoid subsets, each through the isolation of only a limited number of clonal sublines in our study. We feel that the better maintenance of CSCs in the epithelioid sublines may be achieved by some kind of cooperation from the fibroblastoid ones either through cell-cell contacts or mediators released from both subsets, as revealed by the studies of other tumor systems (35, 36, 38). With regard to anchorage-independent colony-formation ability, three out of three epithelioid sublines tested developed colonies in appreciable numbers (512/wells) which was approximately 60% the number of colonies formed by the parental line (889/well). By contrast, none of the three fibroblastoid sublines studied developed any colonies. These observations appeared to be in line with the tumorigenicity results.

The preferential/selective expression of both GRP78 and CD105 in the epithelioid subset of the RCC52 cell line point to the importance of this subset in tumorigenicity, characterized by its ability to display stem/progenitor properties, diverse malignant phenotypes, competence for self-renewal and capacity to differentiate into a heterogeneous tumor cell population (20, 39), as well as to de-differentiate into a clear cell phenotype demonstrated in the present study. CD105 has been identified as a marker for RCC CSCs (18), which are now known to originate from more undifferentiated cells retaining a mesenchymal phenotype but not from the normal CD133⁺ progenitors of the kidney (40, 41). In addition, patients with RCC and low CD133 expression had a higher probability of disease progression and a higher probability of death from cancer (42). On the other hand, the role of CD133 in RCC may be quite different from that of other types of cancer such as lung (43) and pancreatic carcinoma (44). The CD105⁺ cells in a very small number detected are themselves likely to be CSCs, making most of the epithelioid subset of RCC52 cells to serve as the niche for the CSCs. The presence of CD105 in the epithelioid subset is indeed in accordance with our unpublished DNA microarray data in which only the epithelioid subset exhibited expression of the *endoglin* (*CD105*) gene (C-H Hsieh, S-T Pang and S-K Liao). Additionally, these CD105⁺ CSCs can produce not only the epithelial component but also tumor endothelial cells, possibly contributing to intra-tumoral vascularization (45). It would be important to find out whether the CD105⁻ fibroblastoid subset of the sarcomatoid RCC52 cell line

expresses surface CD133. If this is the case, the non-tumorigenic fibroblastoid subset may represent infiltrating resident mesenchymal stem cells as postulated by the same group (45).

The phenotypic differences in the expression of surface E-Cadherin, and cytoplasmic EMA and BCL2 (Table II), and the previously observed genetic differences in the β_2m gene between epithelioid and fibroblastoid sublines (14) make us again hesitant to believe that fibroblastoid cells were the 'M' cells of the EMT transformed directly from the epithelioid cells, *i.e.* from the same cell origin. Careful analysis of the two subsets with molecular cytogenetic approaches including spectral karyotyping and comparative genomic hybridization may help to resolve this issue. Finally, the generality of the observations of the total loss of HLA class I antigens, the presence of both epithelioid and fibroblastoid cell components, and the inducibility of sarcomatoid RCC cells to de-differentiate to clear cell RCC cells *albeit* partially, indeed as the common features for all sarcomatoid RCCs remains to be determined by testing a larger number of cell lines and tumor tissues of sarcomatoid RCCs/clear cell RCCs.

As eluded above, one shortcoming of this study was that the limited number of the epithelioid and fibroblastoid sublines isolated and used might have under-represented the whole spectrum of RCC52 cells. Thus, in the immediate future, it will be important to find ways to identify useful markers for the clear-cut isolation of the whole populations of the epithelioid and fibroblastoid subsets in this RCC52 cell line separately, using agents such as mAbs to as yet identified markers for further analysis. In doing so, one could then confidently confirm or reject the conclusions drawn from the results of the current study based on clonal analysis.

In conclusion, the resulting information of the current study has both immunological (evasion of immune surveillance due to total loss of HLA class I expression) and histopathological (coexistence of the two different subsets) implications. While there are still many questions to be answered, this RCC52 cell line should be valuable for further studies of the pathobiological changes along the lineage of clear cell RCC transformation/progression to sarcomatoid cells, and partial conversion of sarcomatoid RCC to clear cell RCC (transdifferentiation or de-differentiation), in conjunction with the molecular/genetic events associated with EMT, MET (45) and CSCs (35).

Acknowledgements

We wish to thank Tzu-Ju Chang and Chen-Chen Kang for skillful technical assistance. This study was supported by grants from the Chang Gung Medical Research Fund (CMRPD180471, CMRPG380602 and CMRPG3A0231), the National Science Council of Taiwan (NSC94-2314-B-182-060), and the Department of Health of Taiwan (DOH100-TD-C-111-008).

References

- 1 Delahunt B: Sarcomatoid renal carcinoma: the final common dedifferentiation pathway of renal epithelial malignancies. *Pathology* 31: 185-190, 1999.
- 2 Lohse CM and Chevillet JC: A review of prognostic pathologic features and algorithms for patients treated surgically for renal cell carcinoma. *Clin Lab Med* 25: 433-464, 2005.
- 3 Oda H and Machinami R: Sarcomatoid renal cell carcinoma. A study of its proliferative activity. *Cancer* 71: 2292-2298, 1993.
- 4 Skinner DG, Colvin RB, Vermillion CD, Pfister RC and Leadbetter WF: Diagnosis and management of renal cell carcinoma. A clinical and pathologic study of 309 cases. *Cancer* 28: 1165-1177, 1971.
- 5 Tomera KM, Farrow GM and Lieber MM: Well-differentiated (grade 1) clear cell renal carcinoma. *J Urol* 129: 933-937, 1983.
- 6 Akhtar K, Shamsad A, Sufian Z and Tariq M: Sarcomatoid renal cell carcinoma. *Saudi J Kidney Dis Transpl* 22: 120-122, 2011.
- 7 Sella A, Logothetis CJ, Ro JY, Swanson DA and Samuels ML: Sarcomatoid renal cell carcinoma. A treatable entity. *Cancer* 60: 1313-1318, 1987.
- 8 de Peralta-Venturina M, Moch H, Amin M, Tamboli P, Hailemariam S, Mihatsch M, Javidan J, Stricker H, Ro JY and Amin MB: Sarcomatoid differentiation in renal cell carcinoma: A study of 101 cases. *Am J Surg Pathol* 25: 275-284, 2001.
- 9 Chevillet JC, Lohse CM, Zinck H, Weaver AL, Leibovich BC, Frank I and Blute ML: Sarcomatoid renal cell carcinoma: An examination of underlying histologic subtype and an analysis of associations with patient outcome. *Am J Surg Pathol* 28: 435-441, 2004.
- 10 Kwak C, Park YH, Jeong CW, Jeong H, Lee SE, Moon KC and Ku JH: Sarcomatoid differentiation as a prognostic factor for immunotherapy in metastatic renal cell carcinoma. *J Surg Oncol* 95: 317-323, 2007.
- 11 Shuch B, Said J, La Rochelle JC, Zhou Y, Li G, Klatter T, Kabbinaavar FF, Pantuck AJ and Belldegrun AS: Cytoreductive nephrectomy for kidney cancer with sarcomatoid histology-Is up-front resection indicated and, if not, is it avoidable? *J Urol* 182: 2164-2171, 2009.
- 12 Linehan WM, Walther MM and Zbar B: The genetic basis of cancer of the kidney. *J Urol* 170: 2163-2172, 2003.
- 13 Ku JH, Park YH, Myung JK, Moon KC, Kwak C and Kim HH: Expression of hypoxia inducible factor-1 α and 2 α in conventional renal cell carcinoma with or without sarcomatoid differentiation. *Urol Oncol* 29: 731-737, 2011.
- 14 Hsieh CH, Hsu YJ, Chang CC, Liu HC, Chuang KL, Chuang CK, Pang ST, Hasumi K, Ferrone S and Liao SK: Total HLA class I loss in a sarcomatoid renal carcinoma cell line caused by the coexistence of distinct mutations in the two encoding β 2-microglobulin genes. *Cancer Immunol Immunother* 58: 395-408, 2009.
- 15 Liao SK, Meranda C, Avner BP, Romano T, Hussein S, Kimbro B and Oldham RK: Immunohistochemical phenotyping of human solid tumors with monoclonal antibodies in devising biotherapeutic strategies. *Cancer Immunol Immunother* 28: 77-86, 1989.
- 16 Law KS, Chen HC and Liao SK: Non-cytotoxic and sublethal paclitaxel treatment potentiates the sensitivity of cultured ovarian tumor SKOV-3 cells to lysis by lymphokine-activated killer cells. *Anticancer Res* 27: 841-850, 2007.
- 17 Rivoltini L, Cattoretti G, Arienti F, Mastroianni A, Melani C, Colombo MP and Parmiani G: The high lysability by LAK cells of colon-carcinoma cells resistant to doxorubicin is associated with a high expression of ICAM-1, LFA-3, NCA and a less-differentiated phenotype. *Int J Cancer* 47: 746-754, 1991.
- 18 Bussolati B, Bruno S, Grange C, Ferrando U and Camussi G: Identification of a tumor-initiating stem cell population in human renal carcinomas. *FASEB J* 22: 3696-3705, 2008.
- 19 Hendershot LM: The ER function BiP is a master regulator of ER function. *Mt Sinai J Med* 71: 289-297, 2004.
- 20 Chiu CC, Lin CY, Lee LY, Chen YJ, Kuo TF, Chang JT, Liao CT, Wang HM, Yen TC, Shen CR, Liao SK and Cheng AJ: Glucose-regulated protein 78 regulates multiple malignant phenotypes in head and neck cancer and may serve as a molecular target of therapeutic intervention. *Mol Cancer Ther* 7: 2788-2797, 2008.
- 21 Ozcan A, Zhai J, Hamilton C, Shen SS, Ro JY, Krishnan B and Truong LD: PAX2 in the diagnosis of primary renal tumors: Immunohistochemical comparison with renal cell carcinoma marker antigen and kidney-specific cadherin. *Am J Clin Pathol* 131: 393-404, 2009.
- 22 Truong LD and Shen SS: Immunohistochemical diagnosis of renal neoplasms. *Arch Pathol Lab Med* 135: 92-109, 2011.
- 23 Sangoi AR, Karamchandani J, Kim J, Pai RK and McKenney JK: The use of immunohistochemistry in the diagnosis of metastatic clear cell renal cell carcinoma: A review of PAX8, PAX2, hKIM1, RCCma, and CD10. *Adv Anat Pathol* 17: 377-393, 2010.
- 24 Harris SC, Hird PM and Shortland JR: Immunohistochemistry and lectin histochemistry in sarcomatoid renal cell carcinoma: A comparison with classical renal cell carcinoma. *Histopathology* 15: 607-616, 1989.
- 25 DeLong W, Grignon DJ, Eberwein P, Shum DT and Wyatt JK: Sarcomatoid renal cell carcinoma. An immunohistochemical study of 18 cases. *Arch Pathol Lab Med* 117: 636-640, 1993.
- 26 Reuter VE: Sarcomatoid lesions of the urogenital tract. *Semin Diagn Pathol* 10: 188-201, 1993.
- 27 Akhtar M, Tulbah A, Kardar AH and Ali MA: Sarcomatoid renal cell carcinoma: The chromophobe connection. *Am J Surg Pathol* 21: 1188-1195, 1997.
- 28 Kuroiwa K, Konomoto T, Kumazawa J, Naito S and Tsuneyoshi M: Cell proliferative activity and expression of cell-cell adhesion factors (E-Cadherin, α -, β -, and γ -catenin, and p120) in sarcomatoid renal cell carcinoma. *J Surg Oncol* 77: 123-131, 2001.
- 29 Guarino M, Rubino B and Ballabio G: The role of epithelial-mesenchymal transition in cancer pathology. *Pathology* 39: 305-318, 2007.
- 30 Lin JC, Liao SK, Lee EH, Hung MS, Sayion Y, Chen HC, Kang CC, Huang LS and Cherng JM: Molecular events associated with epithelial to mesenchymal transition of nasopharyngeal carcinoma cells in the absence of Epstein-Barr virus genome. *J Biomed Sci* 16: 105, 2009.
- 31 Helfman DM, Kim EJ, Lukanidin E and Grigorian M: The metastasis associated protein S100-A4: Role in tumour progression and metastasis. *Br J Cancer* 92: 1955-1958, 2005.
- 32 Schneider M, Hansen JL and Sheikh SP: S100-A4: A common mediator of epithelial-mesenchymal transition, fibrosis and regeneration in diseases? *J Mol Med* 86: 507-522, 2008.
- 33 De Wever O and Mareel M: Role of tissue stroma in cancer cell invasion. *J Pathol* 200: 429-447, 2003.

- 34 Postlethwaite AE, Keski-Oja J, Moses HL and Kang AH: Stimulation of the chemotactic migration of human fibroblasts by transforming growth factor β . *J Exp Med* *165*: 251-256, 1987.
- 35 Biddle A, Liang X, Gammon L, Fazil B, Harper LJ, Emich H, Costea DE and Mackenzie IC: Cancer stem cells in squamous cell carcinoma switch between two distinct phenotypes that are preferentially migratory or proliferative. *Cancer Res* *71*: 5317-5326, 2011.
- 36 Chen HC, Chou AS, Liu YC, Hsieh CH, Kang CC, Pang ST, Yeh CT, Liu HP and Liao SK: Induction of metastatic cancer stem cells from the NK/LAK-resistant floating, but not adherent, subset of the UP-LN1 carcinoma cell line by IFN- γ . *Lab Invest* *91*: 1502-1513, 2011.
- 37 Celia-Terrassa T, Meca-Cortes O, Mateo F, Martinez de Paz A, Rubio N, Arnal-Estape A, Ell BJ, Bermudo R, Diaz A, Guerra-Rebollo M, Lozano JJ, Estaras C, Ulloa C, Rholvarez-Simon D, Mila J, Vilella R, Paciucci R, Martinez-Balbas M, Garcia de Herrerros A, Gomis RR, Kang Y, Blanco J, Fernandez PL and Thomson TM: Epithelial-mesenchymal transition can suppress major attributes of human epithelial tumor-initiating cells. *J Clin Invest* *122*: 1849-1868, 2012.
- 38 Cameron SR, Dahler AL, Endo-Munoz LB, Jabbar I, Thomas GP, Leo PJ, Poth K, Rickwood D, Guminski A and Saunders NA: Tumor-initiating activity and tumor morphology of HNSCC is modulated by interactions between clonal variants within the tumor. *Lab Invest* *90*: 1594-1603, 2010.
- 39 Li Z: Glucose-regulated protein 78: A critical link between tumor microenvironment and cancer hallmarks. *Biochim Biophys Acta* *1826*: 13-22, 2012.
- 40 Grange C, Tapparo M, Collino F, Vitillo L, Damasco C, Deregibus MC, Tetta C, Bussolati B and Camussi G: Microvesicles released from human renal cancer stem cells stimulate angiogenesis and formation of lung premetastatic niche. *Cancer Res* *71*: 5346-5356, 2011.
- 41 Bussolati B, Brossa A and Camussi G: Resident stem cells and renal carcinoma. *Int J Nephrol* *2011*: 286985, 2011.
- 42 da Costa WH, Rocha RM, da Cunha IW, da Fonseca FP, Guimaraes GC and Zequi Sde C: CD133 immunohistochemical expression predicts progression and cancer-related death in renal cell carcinoma. *World J Urol* *30*: 553-558, 2012.
- 43 Eramo A, Lotti F, Sette G, Pilozi E, Biffoni M, Di Virgilio A, Conticello C, Ruco L, Peschle C and De Maria R: Identification and expansion of the tumorigenic lung cancer stem cell population. *Cell Death Differ* *15*: 504-514, 2008.
- 44 Hermann PC, Huber SL, Herrler T, Aicher A, Ellwart JW, Guba M, Bruns CJ and Heeschen C: Distinct populations of cancer stem cells determine tumor growth and metastatic activity in human pancreatic cancer. *Cell Stem Cell* *1*: 313-323, 2007.
- 45 Kalluri R and Weinberg RA: The basics of epithelial-mesenchymal transition. *J Clin Invest* *119*: 1420-1428, 2009.

Received September 6, 2013

Revised October 18, 2013

Accepted October 22, 2013